ChemCatChem

Research Article
doi.org/10.1002/cctc.202400974

Chemistry Europe
European Chemical Societies Publishing

www.chemcatchem.org

One-Pot Synthesis of (*S*)-Flavanones by a Double-Face Promiscuous Chemo-Enzymatic Cascade of Lipases

Valentina Ubertini,[a] Eliana Capecchi,*[a] Elisabetta Tomaino,[a] Davide Piccinino,[a] Elisa De Marchi,[a] Bruno Mattia Bizzarri,[a] Giovanni Carotenuto,[a] Tiziana Castrignanò,[a] and Raffaele Saladino*[a]

The one-pot stereoselective synthesis of (*S*)-flavanones from 2′-hydroxyacetophenone and substituted aromatic aldehydes was obtained by a double-face promiscuous chemo-enzymatic cascade of porcine pancreas and *Mucor javanicus* lipases. The reaction pathway comprises: A) cross-aldol condensation catalysed by porcine pancreas lipase to yield chalcone intermediates; B) unprecedented intramolecular oxa-Michael addition of chalcone intermediates to (*S*)-flavanones. *Mucor javanicus* lipase was the most effective enzyme in step B. Imidazole and 2-methylimidazole were studied as additive in order to improve the efficacy of the overall transformation. The sustainability of the chemo-enzymatic cascade was increased by immobilization of lipases on cross-linked hydroxy-methylated kraft lignin nanoparticles, by use of concanavalin A. Immobilization conferred considerable stability and reusability at the system for 4 runs. Noteworthy, the reaction mixture was significantly enriched in (*S*)-flavanones under both homogeneous and heterogeneous conditions. Computational studies encompassing docking and molecular dynamic analyses showed the role played by evolutionary conserved oxyanion holes and catalytic triad of *Mucor javanicus* lipase in the stereocontrol of the intra-molecular oxa-Michael addition.

1. Introduction

Enzyme promiscuity unveils the remarkable capacity of enzymes to catalyse non-natural reactions, exhibiting unexpected activities. This interesting behaviour shed light on novel catalytic properties, improving the role of enzymes in green and sustainable chemical and pharmaceutical transformations.[1]

Among promiscuous enzymes, lipases play a pivotal role due to their availability, high stability, and broad range of substrate and high stereo-, chemo- and regioselectivity.[2] In this framework, aldolase activity in the formation of C–C bond has been reported.[3] Examples of application of lipase from porcine pancreas (PPL) in cross-aldol condensations, and their efficacy in the transformation of aromatic aldehydes and aliphatic ketones are discussed in detail, aromatic ketones showing usually low reactivity.[4,5] In this latter case, the chalcone was obtained in low yield.[5] Imidazole derivatives and others *N*-heterocycles are useful additives in order to improve the promiscuous activity of lipases in organic solvents.[6] They are characterized by nucleophilic properties and general acidic and basic catalysis, able to trigger the chemical transformation at the active site of the enzyme.[7] In addition, the electron-rich character of imidazole enables hydrogen bond networks and π–π interactions with amino acids involved in the recognition site of the enzyme.[8]

Flavanones are secondary metabolites with anti-inflammatory, antioxidant, antifibrotic, neuroprotective, antibacterial, and anticancer properties.[9] They are produced in the cell in the (*S*)-enantiomeric pure form by intramolecular cyclization of the corresponding chalcone under the control of chalcone isomerase (CHI, EC 5.5.1.6).[10] The chemical synthesis of flavanones usually requires harsh and tedious multistep procedures, often associated to production of toxic wastes.[11] Bio-catalytic and green pathways can in principle overcome this problem. Despite this, the biotechnology preparation of flavanones is still limited to the scaffold modification of pre-formed flavonoids by yeast extracts.[12] Lipases have not hitherto used in the synthesis of flavanones and no examples are reported in the oxa-Michael addition. On the other hand, lipases can catalyse the formation of C–C, C–S and C–N bonds by inter-molecular Michael addition.[13] In these latter case, the Ser-His-Asp triad and the oxyanion hole of the active site of the enzyme collaborate for the activation of the Michael acceptor, facilitating the correct orientation of the nucleophile.[13a,14] Among lipases, *Mucor javanicus* lipase (MJL) is a low cost enzyme applied in different Michael additions in organic solvents, such as the reaction of pyrimidine and disaccharide acrylates, and of 4-hydroxycoumarin with α,β-unsaturated enones.[15] In addition, MJL showed higher activity than lipase from *Candida antarctica* and PPL in aza-Markovnikov transformation.[16]

We describe here the unprecedented and stereoselective one-pot synthesis of (*S*)-flavanones from aromatic ketones and substituted aldehydes by a double-face promiscuous chemo-

[a] *Dr. V. Ubertini, Dr. E. Capecchi, E. Tomaino, Dr. D. Piccinino, Dr. E. D. Marchi, Dr. B. M. Bizzarri, Dr. G. Carotenuto, Prof. T. Castrignanò, Prof. R. Saladino*
Department of Ecological and Biological Sciences, University of Tuscia, Largo dell'Università snc, 01100 Viterbo, Italy
E-mail: e.capecchi@unitus.it
saladino@unitus.it

Supporting information for this article is available on the WWW under https://doi.org/10.1002/cctc.202400974

enzymatic cascade reaction involving PPL and MJL. In this transformation, MJL catalysed the oxa-Michael addition step. The reaction was performed in iso-octane and dimethyl sulfoxide (DMSO) in the presence of little amounts of distilled water required for the hydration shell of the enzymes.[6b,17] Imidazole derivatives triggered the first step of cross-aldol condensation selectively controlled by PPL.[5] PPL and MJL were mimic of less available and expensive chalcone isomerases.

The sustainability of the chemo-enzymatic cascade was improved by immobilization of PPL and MJL on cross-linked hydroxy-methylated kraft lignin nanoparticles.[18] They increased the performance and stability of lipases, favouring the recovery of the catalytic system and the application for more runs.[19] Overall, the transformation showed excellent atom economy and chemo- and stereoselectivity.

2. Results and Discussion

The one-pot synthesis of flavanones involved the two following steps: (1) formation of chalcones from acetophenone derivatives and substituted aromatic aldehydes by cross-aldol condensation (step A); and (2) intramolecular oxa-Michael addition of chalcones to flavanones (step B). Step A and B were studied alone to optimize the overall transformation.

2.1. Cross-Aldol Condensation (Step A)

The reaction of acetophenone **1** and benzaldehyde **3a** with PPL was studied as a representative example for the synthesis of chalcones. The reaction was performed by addition of PPL (150 mg, 4 KU)[5] and imidazole (ImH1; 1.06 mmol), or in alternative, 2-methylimidazole (ImH2; 1.06 mmol), to equimolar ratio of **1** (1.4 mmol) and **3a** (1.4 mmol) in iso-octane (15.0 mL) at 50 °C for 48 h under argon atmosphere, in order to avoid the auto-oxidation of **3a**.[6b,20] In accordance with previous studies, a large number of PPL units was required to improve the promiscuous activity of the enzyme.[4,5] As a consequence, a large amount of ImH1 and ImH2 was necessary. The efficacy of the reaction was not improved in the presence of higher amount of imidazole. Chalcone **4a** was recovered in 25% and 50% yield, respectively, besides to unreacted substrates, the highest yield being obtained in the presence of ImH2 (Table 1, entry 2 *versus* entry 1). Probably, the high electron-rich character and basicity of ImH2 favoured the aldolase reactivity of PPL.[21] This hypothesis is in accordance with the high catalytic activity in aldol condensation showed by ImH2 when embedded into metal-organic (MOF) architectures.[22] Chalcone **4a** was not obtained in the absence of imidazole derivatives or, in alternative, in the absence of the enzyme (Table 1, entries 3 and 4). Note that the reaction performed in air afforded benzoic acid (not showed) as the only recovered product.[20] No reactivity was observed with *Mucor javanicus* lipase (MJL), suggesting the specialized promiscuous aldolase activity of PPL.[5] The different behaviour of PPL and MJL was not deeply investigated. The low degree of sequence homology of Ser-His-Asp triad in mammalian PPL and microbial MJL may be responsible for the observed results.[13a,23] The scope of the reaction was extended to benzaldehyde derivatives bearing electron withdrawing substituents, *p*-fluorobenzaldehyde **3b**, *p*-chlorobenzaldehyde **3c**, and *p*-bromobenzaldehyde **3d**. The selection of electron withdrawing substituents was due to well-known effect of these substituents in the activation of the aromatic aldehyde acceptor during aldol condensations catalyzed by PPL.[4a] Chalcones **4b--d** were recovered in high yield (Table 1, entries 5–7). The order of reactivity (**3b** > **3c** > **3d**) was in accordance with data previously reported.[24] The procedure was operative also in the case of 2′-hydroxyacetophenone **2** to synthesize 2′-hydroxychalcone derivatives for the intramolecular oxa-Michael addition. The reaction of **2** with **3a--d** afforded chalcones **5a–d** in acceptable yields (Table 1, entries 8–11). In this latter case, the effect of the halogen substituent was not significant in accordance with data previously reported.[24] Structural data of chalcones **4a–d** and **5a--d** are reported in SI 1.

Table 1. Synthesis of chalcones **4a–d** and **5a--d** by cross-aldol condensation of benzaldehyde derivatives and aromatic ketones in the presence of PPL and imidazoles.

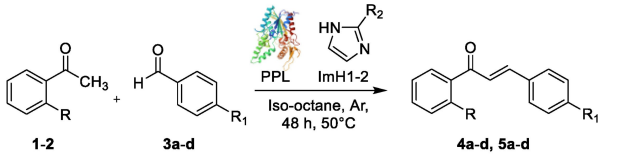

1-2 3a-d 4a-d, 5a-d

1: R=H **2**: R=OH

3a: R_1=H **3b**: R_1=F **3c**: R_1=Cl **3d**: R_1=Br

ImH1: R_2=H ImH2: R_2=CH_3

4a: R=H, R_1=H **4b**: R=H, R_1=F **4c**: R=H, R_1=Cl **4d**: R=H, R_1=Br

5a: R=OH, R_1=H **5b**: R=OH, R_1=F **5c**: R=OH, R_1=Cl **5d**: R=OH, R_1=Br

Entry	Ketone	Aldehyde	ImH	Product	Yield (%)[a]
1	**1**	**3a**	ImH1	**4a**	25
2	**1**	**3a**	ImH2	**4a**	50
3	**1**	**3a**	/	/	/
4	**1**	**3a**	ImH2[b]	/	/
5	**1**	**3b**	ImH2	**4b**	65
6	**1**	**3c**	ImH2	**4c**	62
7	**1**	**3d**	ImH2	**4d**	58
8	**2**	**3a**	ImH2	**5a**	52
9	**2**	**3b**	ImH2	**5b**	55
10	**2**	**3c**	ImH2	**5c**	53
11	**2**	**3d**	ImH2	**5d**	52

[a] Yield was evaluated on the basis of the amount (mmol) of product recovered from the reaction mixture after purification with respect to starting material. [b] No reaction was observed in the absence of lipase. ImH1: imidazole. ImH2: 2-methylimidazole.

2.2. Intramolecular Oxa-Michael Addition (Step B)

No records are available for the promiscuous activity of lipases in the oxa-Michael addition. For this reason, we decided to test the efficacy of both PPL and MJL in the cyclization of **5a** to

flavanone **6a**. Compound **5a** (0.7 mmol) in DMSO (9.0 mL) was treated with the appropriate lipase (PPL and MJL, 2.0 KU) at 50 °C for 48 h under gentle magnetic stirring in the presence of low amount of deionized water (1.0 mL) for the hydration shell of the enzyme.[17,18] DMSO was selected due to the efficacy in the oxa-Michael addition of aromatic aldehydes and aliphatic ketones in the presence α-amylases.[17] Flavanone **6a** was recovered from acceptable to high yield, MJL showing the highest activity (Table 2, entries 1 and 2). Note that MJL was unreactive in cross-aldol condensation step. The procedure was extended to chalcones **5b--d** in the presence of more reactive MJL to afford flavanones **6b–d** in yield of the same order of magnitude than traditional chemical procedures (Table 2, entries 3–5).[25] The synthesis of flavanone **6a** (as a selected case) was also effective under argon atmosphere (Table 2, entry 6), confirming the possibility for step A and step B to occur contemporary in the final enzymatic cascade. Structural data of flavanones **6a--d** are reported in SI 2. The enantiomeric excess (*ee*) of compounds **6a–d** was determined by chiral HPLC analysis as reported in SI 3. The stereochemical behaviour of the reaction is discussed next.

2.3. Synthesis of Flavanones by Homogeneous Chemo-Enzymatic Cascade of PPL and MJL

We evaluated the efficacy of the PPL/MJL chemo-enzymatic cascade in the condensation between 2′-hydroxyacetophenone **2** and benzaldehyde **3a**. Briefly, compounds **2** and **3a** (equimolar ratio; 1.4 mmol) and ImH2 (1.1 mmol) in iso-octane (15.0 mL) and DMSO/deionized water (10 mL; ratio DMSO:H_2O = 9:1) were treated with PPL (4.0 KU) and MJL (2.0 KU) at 50 °C for 48 h under argon atmosphere. The ratio of lipases was selected on the basis of optimal experimental conditions previously determined for step A and step B, respectively, and on the basis of previous studies.[4,5] Flavanone **6a** was obtained in 35% total yield, besides low amount of **5a** and unreacted substrates (Table 3, entry 2). The reaction repeated under similar experimental conditions in the presence of PPL alone (6.0 KU) afforded **5a** in high amount (Table 3, entry 1), confirming the key role of MJL in the intramolecular oxa-Michael addition step. Benzaldehydes **3b--d** were successively used as Michael acceptor to afford flavanones **6b–d** in yield ranging from 35% to 38%, respectively, besides low amount of **5b--d** and unreacted substrate (Table 3, entries 3–5). No specific effect from halogen substituent was observed.[26] Noteworthy, **6a–d** were obtained as prevailing (*S*)-enantiomers (SI 3; original chromatograms from Figures S1 to S4). The stereochemical behaviour of the reaction is discussed next.

Table 2. Synthesis of flavanones **6a–d** from chalcones **5a–d** in the presence of PPL or MJL.

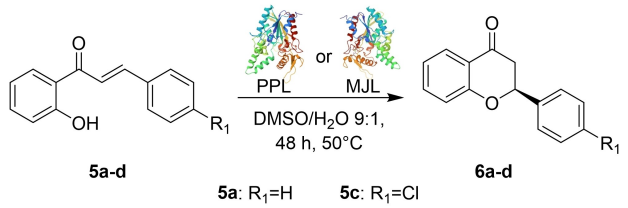

5a-d **6a-d**

5a: R_1=H **5c**: R_1=Cl
5b: R_1=F **5d**: R_1=Br

Entry	Substrate	Enzyme	Product	Yield (%)[a]	ee (%)[b]
1	**5a**	PPL	**6a**	37	/
2	**5a**	MJL	**6a**	70	64
3	**5b**	MJL	**6b**	69	74
4	**5c**	MJL	**6c**	68	72
5	**5d**	MJL	**6d**	67	65
6	**5a**	MJL	**6a**	70	65

[a] Yield was evaluated on the basis of the amount (mmol) of product recovered from the reaction mixture after purification procedure with respect to starting material. [b] Enantiomeric excess (*ee*) was determined by HPLC analysis on a Chiralpak OD-H column.

2.4. Preparation of Heterogeneous Chemo-Enzymatic Cascade of PPL and MJL

We addressed the problem of enzymatic cascade stability and recycling. The efficacy of lignin nanoparticles (LNPs) in the immobilization of lipases is reported.[19a–d,31] In these latter cases, concanavalin A (Con A) was applied as a specific glycoprotein orienting agent, able to favour the tunnelling effect between

Table 3. One-pot synthesis of flavanones **6a–d** from 2′-hydroxyacetophenone **2** and benzaldehyde derivatives **3a–d** by chemo-enzymatic cascade of PPL and MJL under homogeneous conditions.

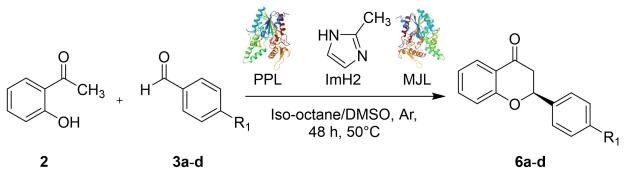

2 **3a-d** **6a-d**

3a: R_1=H **3c**: R_1=Cl
3b: R_1=F **3d**: R_1=Br

Entry	Aldehyde	Enzyme	Product(s)[a]	Yield (%)[b]	ee (%)[c]
1	**3a**	PPL	**6a** (**5a**)	14(28)	/
2	**3a**	PPL/ MJL	**6a**[d] (**5a**)	35(5)	64
3	**3b**	PPL/ MJL	**6b**[e] (**5b**)	38(4)	75
4	**3c**	PPL/ MJL	**6c**[f] (**5c**)	36(5)	72
5	**3d**	PPL/ MJL	**6d**[g] (**5d**)	35(3)	66

[a] Brackets are referred to side-product. [b] Yield was evaluated on the basis of the amount (mmol) of product recovered from the reaction mixture after purification procedure with respect to starting material. [c] Enantiomeric excess (*ee*) was determined by HPLC analysis on a Chiralpak OD-H column. [d] $[\alpha]_D^{20} = -42°$ (c 0.5, $CHCl_3$) [lit. $[\alpha]_D^{20} = -62°$ (c 0.5, $CHCl_3$)] Reference [27]. [e] $[\alpha]_D^{10} = -139.4°$ (c 0.1, $CHCl_3$) [lit. $[\alpha]_D^{10} = -168°$ (c 0.1, $CHCl_3$)], Reference [28]. [f] $[\alpha]_D^{25} = -38.3°$ (c 2.51, $CHCl_3$) [lit. $[\alpha]_D^{25} = -43.7°$ (c 2.51, $CHCl_3$)] Reference [29]. [g] $[\alpha]_D^{24} = -39°$ (c 0.26, EtOH) [lit. $[\alpha]_D^{24} = -47.8°$ (c 0.26, EtOH)] Reference [30].

the active sites of adjacent enzymes.[19d,32] Examples of the beneficial effect of Con A in the control of proximity and orientation during immobilization of enzymes are reported, and the role of the glycoprotein recognition site in the supramolecular interaction was discussed in detail.[32] In addition, hydroxyl-methylation and cross-linking procedures improve the stabilization of LNPs in organic solvents.[18] Hydroxyl-methylated kraft lignin (HKL) was prepared[18b] and characterized in the phenolic sub-units' content by quantitative ^{31}P NMR analyses (SI 4, Table S1).[33] HKL nanoparticles (HKLNPs) were obtained by nanoprecipitation and thermal cross-linking (SI 5). Their morphological characterization, hydrodynamic diameter, poly-dispersion index and ζ- potential, are in SI 5 (Figure S10 and Table S2).[18] The hydrodynamic diameter distribution of HKLNPs was of the same order of amplitude than other lignin nanoparticles prepared in a similar way.[18] **Catalyst I** was obtained by immobilization of PPL (4 KU) and MJL (2 KU) on HKLNPs in the presence of Con A as a molecular spacer. Briefly, Con A (30 mg) in PBS (15 mL) was deposited on HKLNPs (60 mg) in PBS (15 mL) under gentle sonication for 5 min at room temperature to afford HKLNPs/Con A intermediate (Scheme 1). Next, PPL (4 KU) and MJL (2 KU) in PBS (30 mL) were added to HKLNPs/Con A intermediate in PBS, and the mixture was stirred at 4 °C for 24 h.[19a–b,d] The suspension was centrifuged and washed two times with PBS to afford **Catalyst I** in 98% yield. A schematic representation of **Catalyst I** in which Con A contemporary supports MJL and PPL is reported in Scheme 1 as a working hypothesis. Confocal analysis of **Catalyst I** in the presence of labelled PPL (FITC-PPL, green) and MJL (Rhodamine B-MJL, red) (Figure S11) showed that lipases < are localized in proximity (experimental details for the labelling procedure are in SI 6).

Field emission scanning electron microscopy (FE-SEM) showed nanoparticles with regular spherical shape characterized by the typical corona-like structural motif associated to Con A (Figure 1, panel A).[19d,32d] Dynamic light scattering (DLS) analysis is reported in Figure 1 (panel B) in comparison with HKLNPs (Figure S10, Panel B). **Catalyst I** showed an average diameter of 283 nm higher than HKLNPs (107 nm). Note that, the average diameter of **Catalyst I** increased of c.a. 170 nm with respect to starting nanoparticle (Figure S10) after the deposition of Con A, PPL and MJL. This result was in accordance with previous data.[32d] The ζ- potential value of **Catalyst I** was −6.02 mV, similar to that of HKLNPs (−10.15 mV).

The immobilization parameters of **Catalyst I** were evaluated as reported in Equations (1) and (2).

$$\text{Immobilization yields } (\%) = [(U_a \quad -U_r)/U_a]x100 \tag{1}$$

$$\text{Activity } (\text{units/mg}) = U_x/mg_{support} \tag{2}$$

Where U_x are the units of immobilized enzyme, U_a are the total units of the enzyme added to the solution, and U_r are the residual units of the enzyme in the washing solution.

The activity parameters were measured by the standard *para*-nitrophenol assay.[34] In a typical experiment, **Catalyst I** (1.5 mg/mL in PBS) was added to p-nitrophenyl laurate (20 mM) in Tris-HCl at 25 °C. The international unit of lipase activity was defined as the amount of enzyme necessary to hydrolyse 1.0 μmol of p-NPL in 1 min at 25 °C and optimal pH. Immobilization yield of lipases was 98%, while the overall activity of **Catalyst I** was 94 U/mg. Note that, PPL and MJL were immobilized in the optimal 2:1 ratio, in accordance with the relative amount of the two enzymes applied under homogeneous conditions.

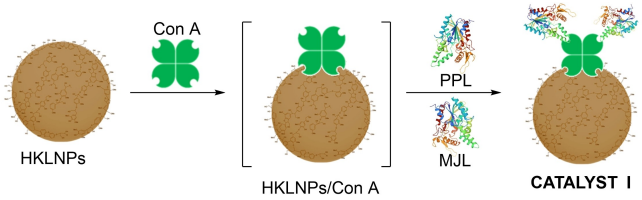

Scheme 1. Preparation of **Catalyst I**. Con A was used as a molecular spacer.

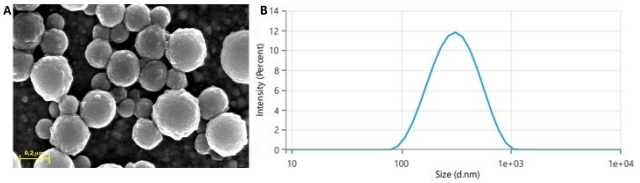

Figure 1. Panel A: FE-SEM images of **Catalyst I**. Panel B: DLS size analysis.

2.5. Synthesis of Flavanones by Heterogeneous Chemo-Enzymatic Cascade of PPL and MJL

Compounds **2** (1.4 mmol) and **3a–d** (1.4 mmol) and ImH2 (1.1 mmol) were treated with **Catalyst I** (64 mg, 6 KU) at 50 °C for 48 h in the biphasic system iso-octane (15.0 mL) and DMSO/deionized water (10 mL) under argon atmosphere. Under these experimental conditions, flavanones **6a–d** were isolated from acceptable to high yield (Table 4, entries 1–4) besides unreacted substrates and traces of **5a–d**. **Catalysts I** was more active than the homogeneous mixture of native lipases (Table 4 *versus* Table 3), probably due to the occurrence of stability and tunnelling effect in the enzymatic cascade.[35] The reactivity of **Catalyst I** was retained for at least 4 runs in the case of **6a** (Table 4, entries 5–8), confirming the reusability of the enzymatic cascade for more transformations. Again, the reaction was stereoselective, and flavanones **6a--d** were isolated as (*S*)-enantiomers in enantiomeric excess higher than that previously observed for homogeneous conditions (Table 4) (SI 3; original chromatograms from Figures S5 to S8). Note that *ee* was retained during recycling of **Catalyst I**.

2.6. Stereochemical Behaviour and Computational Analysis

Flavanones **6a--d** were isolated under homogeneous conditions as (*S*)-enantiomer with 64%–75% *ee* (Table 3, entries 2–5). This trend was in accordance with the selectivity pattern of chalcone

Table 4. Multienzymatic cascade for the one-pot synthesis of flavanones **6a--d** under heterogeneous conditions.

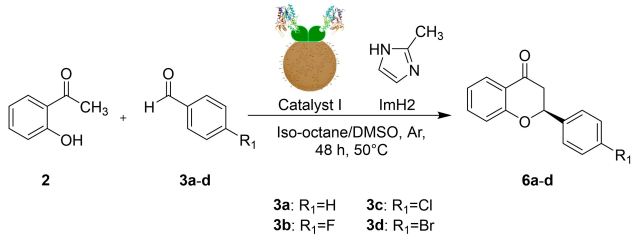

Entry	Aldehyde	Product	Yield (%)[a]	ee (%)[b]
1	**3a**	**6a**[c]	42	84
2	**3b**	**6b**[d]	45	92
3	**3c**	**6c**[e]	44	89
4	**3d**	**6d**[f]	42	87
5	**3a**	**6a**	40 (Run n.1)	84
6	**3a**	**6a**	38 (Run n.2)	83
7	**3a**	**6a**	37 (Run n.3)	83
8	**3a**	**6a**	34 (Run n.4)	84

[a] Yield was evaluated on the basis of the amount (mmol) of product recovered from the reaction mixture after purification procedure with respect to starting material. [b] Enantiomeric excess (*ee*) was determined by HPLC analysis on a Chiralpak OD-H column. [c] $[\alpha]_D^{20} = -56.7°$ (c 0.5, $CHCl_3$) [lit. $[\alpha]_D^{20} = -62°$ (c 0.5, $CHCl_3$)] Reference [27]. [d] $[\alpha]_D^{10} = -162.6°$ (c 0.1, $CHCl_3$) [lit. $[\alpha]_D^{10} = -168°$ (c 0.1, $CHCl_3$)], Reference [28]. [e] $[\alpha]_D^{25} = -47°$ (c 2.51, $CHCl_3$) [lit. $[\alpha]_D^{25} = -43.7°$ (c 2.51, $CHCl_3$)] Reference [29]. [f] $[\alpha]_D^{24} = -52.3°$ (c 0.26, EtOH) [lit. $[\alpha]_D^{24} = -47.8°$ (c 0.26, EtOH)] Reference [30].

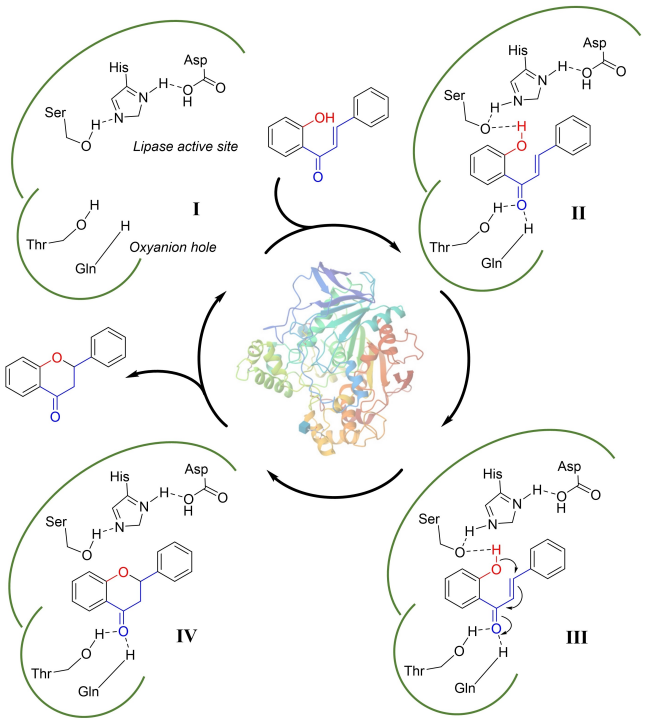

Scheme 2. Proposed mechanism for lipase mediated oxa-Michael addition.

isomerases in the cyclization of chalcone to flavanone, and with previously results reported for the intermolecular Michael addition of cyclohexanone and acetyl-acetone.[10b,d,13b] No data are available for the stereochemistry of the intramolecular oxa-Michael addition in the presence of lipases. The possibility that ImH2 could act as base to promote racemization process was ruled out by the fact that similar *ee* values were obtained in the synthesis of **6a–d** in the presence (Table 3) or absence (Table 2) of imidazole derivatives. Accordingly, **6a** suspended in DMSO/H_20 at 50 °C for 48 h in the presence of ImH2 retained the original *ee* value.

The reaction pathway for the synthesis of **6a** is schematically described in Scheme 2 as an adaptation of the hypothesis previously reported for the aza-Michael addition catalysed by lipase B from *Candida antarctica*.[14] It involves the coordination of **5a** with the oxyanion hole of the enzyme (Thr and Gln), followed by nucleophilic activation of the 2′-hydroxy group by Ser-His-Asp triad and successive intramolecular oxa-Michael addition.[14] Note that, the oxyanion hole and the Ser-His-Asp triad are highly conserved amino acid residues in the lipase family.[36]

Computational studies were performed in order to rationalize the observed (*S*)-stereochemistry. Since crystallographic data of MJL are not available, the tertiary structure of the enzyme was predicted by combining four molecular modelling programs, namely Modeller, AlphaFold2, RoseTTAFold, and I-TASSER.[22,37–40] In addition, PROCHECK, ERRAT, and VERIFY-3D, were used to validate the predicted structures.[41–43] The detailed description of the simulation process is reported in SI 7. Among the tested programs, RoseTTAFold furnished the best 3-dimensional structure model, 2.R, as further confirmed by ProSA-web and QMEANBrane server (Table S3).[44,45] The predicted structure falls perfectly within the mean for proteins with a similar number of residues (ProSA-web), showing no critical regions (Figure S12, Panel B). To confirm the accuracy of model 2.R, the stability of the structure was successively analysed in water by a long molecular dynamics' simulation (1 μs; GROMACS software, SI 8).[46] The root mean square deviation (RMSD) of the alpha-carbon atoms from the initial conformation of the protein was considered. The protein deviates from the initial structure for the first 220 ns, then undergoes a sudden drop for another 50 ns, until reaching a plateau at 280 ns (RMSD, 0.75 ± 0.09 nm). The initial structural drift left to a potential energy minimum for the remainder of the simulation (Figure S13, Panel A). The average value of Solvent Accessible Surface Area (SASA) was 202 ± 6 nm^2 (Figure S13, Panel B), and it was constant during the simulation, suggesting that the variation of RMSD in the structural settling phase was probably due to the reorganization of intra-chain molecular interactions in the non-surface-exposed region. The radius of gyration (Rg) was also investigated (Rg was 2.136 ± 0.020 nm), indicating strong structural stability (Figure S13, Panel C). The region comprising residues 32–55 (red) showed the highest RMSF peak corresponding to the LID domain of MJL, which is a regulatory domain for the catalytic site.[2b] Residues 76–79 and 98–108 (yellow) showed greater flexibility compared to the rest of the protein, while the region comprising residues 80–97 (lilac) was composed by α-

helix and showed no marked flexibility. Residues 123–131 form a loop (magenta) connecting the α-helix of the previously described domain to the "Rossmann fold" architecture (Figure 2).

Next, we performed the molecular docking of **5a** in the predicted catalytic site of the enzyme. CASTp software was used in order to identify the binding pocket and the amino acids involved in the coordination.[47] Ser188, Asp189, Thr190, Thr210, Ser216, Asp219, Gln221, Asp223, His236, Ser242, His271, and Gln277 were identified in the enzyme-substrate interaction. The exploration of the stereochemistry was performed by docking software Autodock Vina.[48] 200 molecular docking simulations were calculated by comparison of **5a** in the optimal conformation for the S-ring closure with the corresponding R-ring closure counterpart (Figure 3). The docking data (best poses) were obtained by PLIP software (SI 9).[49] As reported in Table S4, 5a formed only one hydrogen bond with Gln277 (3.176 ± 0.018 Å) in all trials (N.100) analysed for the R-ring closure (Figure 3, Panel B), probably due to the steric hindrance of the aromatic moiety with the bulky of the enzyme, maintaining high mobility within the catalytic pocket. In contrast, **5a** formed two hydrogen bonds with Gln277 (2.808 ± 0.004 Å) and Ser216 (3.27 ± 0.17 Å) in 21% of the trials when arranged for the S-ring closure (Figure 3, Panel A). Note that, Thr residue was not involved in the coordination of the carbonyl moiety of chalcone. This pattern was different from that previously hypothesized for lipase from *Candida antarctica*[14b]. The Gibbs free energy of **5a** was calculated by steered molecular dynamics (SMD) analyses with umbrella sampling, exploiting the relationships between $\triangle G$ and the work done to force the system along a path from A to B (*WAB*) by the following equation:

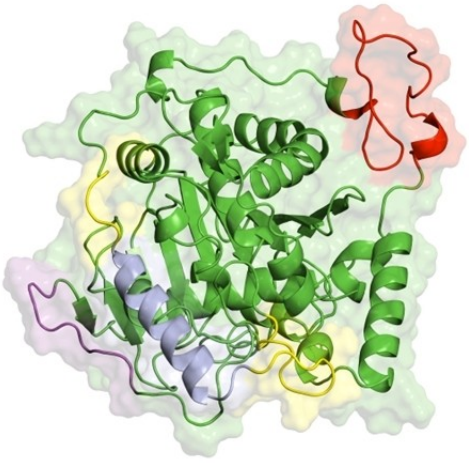

Figure 2. Figure highlighting the various regions showing greater fluctuation in the RMSF: residues 32–55 in red, LID domain; residues 76–79 and 98–108 in yellow; residues 80–97 in light blue, α-helix; residues 123–131 in magenta, loop connecting the α-helix to the Rossmann fold.

$$\Delta G_{AB} = -kBT\ log(e^{-\beta WAB}) \quad (3)$$

Where angle brackets indicate the average over a canonical ensemble of the initial state A, and $\beta = 1/kBT$.[50] Details of SMD are in SI 10. In addition, CAVER 3.0 software (PyMOL) was used to find the most suitable direction of the harmonic oscillator (Figure S14, Panel A).[51] From each simulation, the potential mean force (PMF) was extracted by the Weighted Histogram Analysis Method (WHAM) included in GROMACS (Figure S14, Panel B). The obtained Gibbs free energy values for ligand insertion were −4.19 ± 1.15 kcal/mol for **5a** in the conformation for the S-ring closure, and −3.35 ± 0.97 kcal/mol in the R-ring closure counterpart. Overall, computational analysis confirmed the prevalence of the ring-closure of **5a** to yield (*S*)-flavanone.

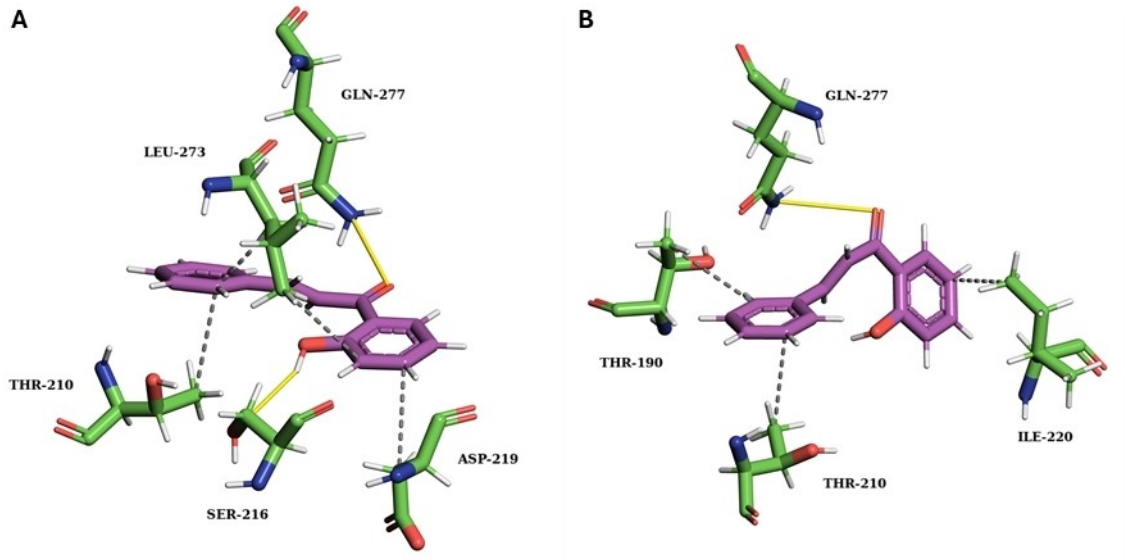

Figure 3. Panel A: Interactions of **5a** with the active site of MJL in the optimal conformation for the S-ring closure. Hydrophobic interactions are represented by dashed grey lines and hydrogen bonds by yellow lines. Panel B: Interactions of **5a** with the active site of MJL in the optimal conformation for the R-ring closure.

Noteworthy, the stereoselectivity of the reaction was improved in the presence of **Catalyst I**, in which case flavanones **6a–d** were isolated as (*S*)-enantiomer with 84%–92% *ee* (Table 4, entries 1–4).

3. Conclusions

We demonstrated that PPL and MJL work as a double-face promiscuous chemo-enzymatic cascade for the one-pot synthesis of (*S*)-flavanones from aromatic ketones and aromatic aldehydes. PPL selectively mediated the cross-aldol condensation, while MJL was the most effective enzyme in the intramolecular oxa-Michael addition. The scope of the reaction was extended from homogeneous to heterogeneous conditions by immobilization of lipases on hydroxyl-methylated and cross-linked lignin nanoparticles resistant to organic solvent, in the presence of Concanavalin A as a proximity orienting spacer. The yield of flavanones was higher under heterogeneous conditions than homogeneous counterpart, confirming the beneficial role of the immobilization procedure. Noteworthy, (*S*)-flavanones were obtained as the prevailing stereoisomers. This stereoselectivity was in accordance with the reaction pattern of chalcone isomerases.[10] The computational analysis, performed after modelling the MJL active site involved in the stereoselective intramolecular oxa-Michael addition, showed the key role played by highly conserved oxyanion hole and Ser-His-Asp triad in the stabilization of the chalcone intermediate for the S-ring closure. The enantiomeric excess of (*S*)-flavanones increased after immobilization of the enzymatic cascade. Even if computational analyses were not performed in this latter case, examples of increased stereoselectivity of lipases after immobilization procedure are reported, due to beneficial modification of the enzyme shape and features at the active site.[52] Lipase from porcine pancreas immobilized on commercial DEAE-Sepharose displayed enantioselectivity higher than the free enzyme in the resolution of glycidyl butyrate,[53] and lipase from *Candida rugose* and from *Candida antarctica* improved their enantioselectivity after immobilization on aminated supports.[54] Overall, the use of commercially available and low cost lipases instead of chalcone isomerases, the high atom economy associated to the enzymatic cascade and the limitation of tedious purification steps and chemical reagents, associated to the high stereoselectivity and recoverability of the heterogeneous biocatalyst, highlighted PPL and MJL enzymatic cascade as a green alternative to conventional procedures for the one-pot synthesis of (*S*)-flavanones.

Experimental Section

Material and Methods

Acetophenone, benzaldehyde, imidazole, 2-methyl-imidazole, *p*-fluorobenzaldehyde, *p*-chlorobenzaldehyde, *p*-bromobenzaldehyde, 2′-hydroxyacetophenone, lipase from porcine pancreas (PPL 30 U/mg), lipase M from *Mucor javanicus* (MJL, 300 U/mg), concanavalin A (Con A) type IV from *Canavalia ensiformis* (Jack bean), 4-nitrophenyl palmitate and formaldehyde, were purchased from Sigma-Aldrich. Kraft lignin was purchased from Stora Enso. Organic solvents were purchased from Sigma-Aldrich and were used without further purification. Sodium phosphate buffer (PBS 0.1 M, pH 7) was prepared by using MilliQ water. Spectrophotometric analysis was performed with Cary 60 UV-Vis spectrophotometer equipped with a single cell peltier thermostated holder. Chemical reactions were monitored by using thin layer chromatography on pre-coated aluminium silica gel Merck 60 F254 plates and UV lamp (λ_{max} = 254 nm) for visualization. ^{1}H NMR and ^{13}C NMR spectra were recorded on a Bruker (400 MHz) spectrometer using $CDCl_3$. Chemical shifts (δ) are expressed in parts per million (ppm). Coupling constants J are expressed in hertz (Hz). Spin multiplicities are given as s (singlet), d (doublet), dd (doublet of doublets), and m (multiplet). MS data were obtained by using LC/MS Agilent 1100 LC–MSD VL system (G1946 C) interfaced with an ESI source (spray voltage of 4.5 kV and nitrogen as sheath gas). HPLC measurements were performed using an Ultimate 3000 Rapid Resolution UHPLC system (ThermoFisher scientific) equipped with a Daicel Chiralpak OD–H column and a multiwavelength detector. Optical rotations were measured by Anton Paar MCP 4100 Polarimeter at λ = 589 nm.

Cross-Aldol Condensation (Step A)-General Procedure

The reactions were performed with ketones **1–2** (1.4 mmol) and aldehydes **3a–d** (1.4 mmol) in iso-octane (15.0 mL) in the presence of PPL (150 mg, 4 KU) and 2-methyl-imidazole (ImH2; 1.06 mmol), at 50 °C for 48 h under argon atmosphere.[5,6b,20] The reactions were monitored by thin layer chromatography (TLC, *n*-hexane/EtOAc = 9.0 : 1.0) developed with phosphomolybdic acid. At the end, the reactions were diluted with deionized water to remove the suspended solid enzyme and ImH2. The organic layer was separated, washed with deionized water, and carefully evaporated under reduced pressure. The crude was dissolved in MeOH (2 mL) and kept at 4 °C overnight. The chalcones were isolated as crystals after filtration, washed carefully with ice water and cold MeOH to neutral reaction, and further purified by crystallization.[55] The original ^{1}H NMR and ^{13}C NMR spectra of chalcones are in SI 1.

Intramolecular Oxa-Michael Addition (Step B)-General Procedure

The reactions were performed with chalcones **5a–d** (0.7 mmol) in DMSO (9.0 mL) and deionized water (1.0 mL) in the presence of MJL (2.0 KU) at 50 °C for 48 h under gentle magnetic stirring.[17,18] The reactions were monitored by thin layer chromatography (TLC, n-hexane/EtOAc = 9.0 : 1.0). At the end, the organic phase was separated, and the organic solvent was evaporated under reduced pressure. The resulting flavanones were purified by flash chromatography. The original ^{1}H NMR and ^{13}C NMR spectra of flavanones are in SI 2.

Synthesis of flavanones by homogeneous chemo-enzymatic cascade of PPL and MJL-General procedure. The reactions were performed with ketone 2 (1.4 mmol) and aldehydes **3a–d** (1.4 mmol) and ImH2 (1.1 mmol) in iso-octane (15.0 mL) and DMSO/deionized water (10 mL; ratio DMSO: H_2O = 9 : 1), by addition of PPL (4.0 KU) and MJL (2.0 KU). The reaction was stirred at 50 °C for 48 h under argon atmosphere.[5,6b,17–18,20] At the end, the organic phase was separated, and the organic solvent was evaporated under reduced pressure. The resulting flavanones were purified by flash chromatography. The original ^{1}H NMR and ^{13}C NMR spectra of flavanones are in SI 2.

Preparation of Catalyst I-General Procedure

For the preparation of Catalysts I, 15 mL of Con A solution (2.0 mg/mL) in PBS (0.1 M, pH 7.0) were added to 15 mL of HKLNPs (4.0 mg/mL) in PBS (0.1 M, pH 7.0) under gentle sonication conditions for 5 min at room temperature to afford HKLNPs/Con A intermediate. Next, PPL (4 KU) and MJL (2 KU) dissolved in PBS (30 mL, 0.1 M, pH 7.0) were added to HKLNPs/Con A intermediate, and the mixture was stirred at 4 °C in orbital shaking for 24 h.[19a–b,d] The suspension was centrifuged (14339 RCF, 4 °C for 10 min) and washed two times with PBS (0.1 M, pH 7.0) to afford Catalyst I in 98 % yield.

Synthesis of Flavanones by Heterogeneous Chemo-Enzymatic Cascade of PPL and MJL-General Procedure

The reactions were performed with ketone 2 (1.4 mmol) and aldehydes **3 a–d** (1.4 mmol) and ImH_2 (1.1 mmol) in iso-octane (15.0 mL) and DMSO/deionized water (10 mL; ratio DMSO: H_2O = 9 : 1), by addition of Catalyst I (64 mg, 6 KU). The reaction was stirred at 50 °C for 48 h under argon atmosphere.[5,6b,17–18,20] At the end, the reaction was filtered to recover Catalyst I, the organic phase was separated, and the organic solvent evaporated under reduced pressure. The resulting flavanones were purified by flash chromatography. The original ^{1}H NMR and ^{13}C NMR spectra of flavanones are in SI 2.

Computational Analysis-General Procedure

Modeller 10.5, AlphaFold2, RoseTTAFold, and I-TASSER prediction software tools were employed.[37–40] The quality of produced models was evaluated by ERRAT, PROCHECK, and VERIFY-3D.[41–43] The optimal model was further analysed with the following tools: (1): ProSA-web to evaluate the free energy difference between MJL and reference proteins with known 3D structures; and (2): QMEANBrane to verify the water solubility and globular properties.[44,45] GROMACS software (version 2023.3) was used with the "charmm36-jul2022" force field, for molecular dynamics (MD) study and trajectory analysis.[46,56] Chalcone topologies were generated with CharmGUI software, which incorporates the Charm atomic definitions.[57] The initial structures for MD simulation were based on predicted MJL model in the presence of chalcone and optimized by molecular docking. The systems were cantered within a simulation box and solvated using the TIP3P water model.[58] A standard protocol for the production of the molecular dynamics trajectory was used. The energy minimization employed the steepest descent method, setting a limit of 50,000 steps and terminating when forces decreased to below 1000 kJ/mol/nm. An NVT equilibration phase was applied, lasting 1 ns at a constant temperature of 300 K, employing the V-rescale algorithm. Subsequently, NPT equilibration phase of 2 ns was performed, utilizing the Parrinello-Rahman pressure coupling with pressure set at 1 bar. The particle mesh Ewald method was used to handle long-range electrostatic interactions within the system. The solvated protein was then subjected to 1 μs production MD simulation, using a time-step of 2 fs. All the MD simulations were performed on the Tier-0 Leonardo Supercomputer of the Cineca Consortium (leonardo supercomputer.cineca.eu/ffplus-innovation-in-industry).[59] The identification of the binding pocket was performed using the software CASTp.[47] Molecular docking was carried out using AutoDock Vina 1.1.2.[48] The binding interactions were analyzed by the PLIP software.[49,60] The calculation of the binding free energy was carried out through steered molecular dynamics with umbrella sampling.[50] This protocol was implemented using the CAVER 3.0 plugin for PyMOL (The PyMOL Molecular Graphics System, Version 2.5.4 Schrödinger, LLC) and GROMACS with the gmx wham module.[51]

4. Supporting Information Summary

SI 1. ^{1}H NMR and ^{13}C NMR spectra of chalcones **4 a**--**d** and **5 a**–**d**. SI 2. ^{1}H NMR and ^{13}C NMR spectra of compounds **6 a**–**d**. SI 3. Chiral HPLC analysis of compounds **6 a**–**d**. SI 4. Preparation and structural characterization of HKL. SI 5. Preparation and structural characterization of HKLNPs. SI 6. Labelling procedure and confocal analysis of **Catalyst I**. SI 7. 3D MJL Model. SI 8. Stability of the 3D MJL Model. SI 9. Docking analysis. SI 10. SMD analysis of Gibbs free energy. The authors have cited additional references within the Supporting information (Ref. [61–67]).

Acknowledgements

Acknowledgements Text. Progetto ECS Rome Technopole-PNRR Missione 4 Componente 2 Investimento 1.5, finanziato dall'Unione Europea–Next Generation EU. Open Access publishing facilitated by Università degli Studi della Tuscia, as part of the Wiley - CRUI-CARE agreement.

Conflict of Interests

The authors declare no conflict of interest.

Data Availability Statement

The data that support the findings of this study are available in the supplementary material of this article.

Keywords: Enzymatic cascade · Lipase promiscuity · Flavanones · Chalcones · Lignin nanoparticles

[1] a) G. Rix, E. J. Watkins-Dulaney, P. J. Almhjell, C. E. Boville, F. H. Arnold, C. C. Liu, *Nat. Commun.* **2020**, *11*, 5644; b) R. B. Leveson-Gower, C. Mayer, G. Roelfes, *Nat. Chem. Rev.* **2019**, *3*, 687.
[2] a) F. Hasan, A. A. Shah, A. Hameed, *Biotechnol. Adv.* **2009**, *27*, 782–798; b) S. Hari Krishna, N. G. Karanth, *Catal. Rev.* **2002**, *44*, 499–591; c) R. D. Schmid, R. Verger, *Angew. Chem. Int. Ed.* **1998**, *37*, 1608–1633.
[3] a) B. P. Dwivedee, S. Soni, M. Sharma, J. Bhaumik, J. K. Laha, U. C. Banerjee, *ChemistrySelect* **2018**, *3*, 2441–2466; b) C. Li, X.-W. Feng, N. Wang, Y.-J. Zhou, X.-Q. Yu, *Green Chem.* **2008**, *10*, 616–618.
[4] a) Z. Xie, N. Wang, L. Zhou, F. Wan, T. He, Z. Le, X.-Q. Yu, *ChemCatChem* **2013**, *5*, 1935–1940; b) D. González-Martínez, V. Gotor, V. Gotor-Fernández, *Eur. J. Org. Chem.* **2016**, 1513–1519.
[5] Y. N. Mitrev, A. Y. Mehandzhiyski, D. I. Batovska, A. Liese, B. Galunsky, *J. Serb. Chem. Soc.* **2016**, *81*, 1231–1237.
[6] a) B. K. Liu, Q. Wu, J. M. Xu, X. F. Lin, *Chem. Commun.* **2007**, *3*, 295–297; b) X. Chen, B. K. Liu, H. Kang, X. F. Lin, *J. Mol. Catal. B* **2011**, *68*, 71–76.
[7] a) E. B. Anderson, T. E. Long, *Polymer* **2010**, *51*, 2447–2454; b) A. Richaud, N. Barba-Behrens, F. Méndez, *Org. Lett.* **2011**, *13*, 972–975; c) L. Zhang, X.-M. Peng, G. L. V. Damu, R.-X. Geng, C.-H. Zhou, *Med. Res. Rev.* **2014**, *34*, 340–437; d) S. S. Alghamdi, R. S. Suliman, K. Almutairi, K. Kahtani, D. Aljatli, *Drug Des. Dev. Ther.* **2021**, *15*, 3289–3312; e) H. V. Tolomeu, C. A. M. Fraga, *Molecules* **2023**, *28*, 838; f) E. Marcantonio, D. Guazzetti, K. Bugatti, L. Battistini, A. Sartori, G. Pelosi, C. Curti, F. Zanardi, *Chem. Eur. J.* **2023**, *29*, e202301200.
[8] T. Fu, S. Smith, M. Camarasa-Gómez, X. Yu, J. Xue, C. Nuckolls, F. Evers, L. Venkataraman, S. Wei, *Chem. Sci.* **2019**, *10*, 9998–10002.
[9] a) H. Tutunchi, F. Naeini, A. Ostadrahimi, M. J. Hosseinzadeh-Attar, *Phytother. Res.* **2020**, *34*, 3137–3147; b) Y. Q. Hua, Y. Zeng, J. Xu, X. L. Xu,

Phytomedicine **2021**, *81*, 153412; c) Y. Du, J. Ma, Y. Fan, X. Wang, S. Zheng, J. Feng, J. Li, Z. Fan, G. Li, Q. Ye, *Oxid. Med. Cell Longev.* **2021**, 1210675; d) L. Zou, M. Ning, W. Wang, Y. Zheng, L. Ma, J. Lv *Drug Des. Dev. Ther.* **2020**, *14*, 5469–5482; e) S. Zhang, D. D. Li, F. Zeng, Z. H. Zhu, P. Song, M. Zhao, J. A. Duan, *Nat. Prod. Res.* **2019**, *33*, 1756–1760; f) X. Shi, X. Luo, T. Chen, W. Guo, C. Liang, S. Tang, J. Mo, *J. Cell. Mol. Med.* **2021**, *25*, 2563–2571.

[10] a) N. A. A. Elkanzi, H. Hrichi, R. A. Alolayan, W. Derafa, F. M. Zahou, R. B. Bakr, *ACS Omega* **2022**, *7*, 27769–27786; b) J. M. Jez, J. P. Noel, *J. Biol. Chem.* **2002**, *277*, 1361–1369; c) A. M. Pereira, H. Cidade, M. E. Tiritan, *Molecules* **2023**, *28*, 426; d) J. J. Ruiz-Pernía, E. Silla, I. Tuñón, *J. Phys. Chem. B.* **2006**, *110*, 20686–92.

[11] a) C. M. Brennan, I. Hunt, T. C. Jarvis, C. D. Johnson, P. D. McDonnell, *Can. J. Chem.* **1990**, *68*, 1780–1785; b) K. Tanaka, T. Sugino, *Green Chem.* **2001**, *3*, 133–134; c) B. S. Goud, K. Panneerselvam, D. E. Zacharias, G. R. Desirajua, *J. Chem. Soc.-Perkin Trans.* **1995**, *2*, 325–330; d) D. Kumar, G. Patel, A. K. Kumar, R. Roy, *J. Heterocycl. Chem.* **2009**, *46*, 791–795; e) S. H. Son, Y. Y. Cho, H.-S. Yoo, S. J. Lee, Y. M. Kim, H. J. Jang, D. H. Kim, J.-W. Shin, N.-J. Kim, *RSC Adv.* **2021**, *11*, 14000–14006; f) J. P. Marais, D. Ferreira, D. Slade, *Phytochemistry* **2005**, *66*, 2145–76; g) L. Wang, X. Liu, Z. Dong, X. Fu, X. Feng, *Angew. Chem. Int. Ed.* **2008**, *47*, 8670–8673; h) M. M. Biddle, M. Lin, K. A. Scheidt, *J. Am. Chem. Soc.* **2007**, *129*, 3830–3831; i) D. Zhao, B. Beiring, F. Glorius, *Angew. Chem. Int. Ed.* **2013**, *52*, 8454–8458.

[12] a) T. Janeczko, M. Dymarska, M. Siepka, R. Gniłka, A. Lesniak, J. Popłonski, E. Kostrzewa-Susłow, *J. Mol. Catal. B* **2014**, *109*, 47–52; b) Y. Kawada, T. Goshima, R. Sawamura, S.-I. Yokoyama, E. Yanase, T. Niwa, A. Ebihara, M. Inagaki, K. Yamaguchi, K. Kuwata, *J. Biosci. Bioeng.* **2018**, *126*, 301–309; c) X. Liu, J. Yang, L. Gao, L. Zhang, X. Lei, *Biotechnol. J.* **2020**, *15*, 2000119; d) I. L. de Matos, W. G. Birolli, D. D. A. Santos, M. Nitschke, A. L. M. Porto, *J. Mol. Catal.* **2021**, *513*, 111734.

[13] a) G. A. Strohmeier, T. Sović, G. Steinkellner, F. S. Hartner, A. Andryushkova, T. Purkarthofer, A. Glieder, K. Gruber, H. Griengl, *Tetrahedron* **2009**, *65*, 5663–5668; b) J. -F. Cai, Z. Guan, Y.-H. He, *J. Mol. Catal. B* **2011**, *68*, 240–244; c) P. V. S. Rizzo, L. A. Boarin, I. O. M. Freitas, R. S. Gomes, A. Beatriz, A. W. Rinaldi, N. L. C. Domingues, *Tetrahedron Lett.* **2014**, *55*, 430–434; d) M. A. Ortega-Rojas, J. D. Rivera-Ramirez, C. G. Àvila-Ortiz, E. Juaristi, F. González-Muñoz, E. Castillo, J. Escalante, *Molecules* **2017**, *22*, 2189.

[14] a) A. Patti, C. Sanfilippo, *Int. J. Mol. Sci.* **2022**, *23*, 2675; b) B. Gu, Z.-E. Hu, Z.-J. Yang, J. Li, Z.-W. Zhou, N. Wang, X.-Q. Yu, *Chem. Sel.* **2019**, *4*, 3848–3854; c) P. Carlqvist, M. Svedendahl, C. Branneby, K. Hult, T. Brinck, P. Berglund, *ChemBioChem* **2005**, *6*, 331–336.

[15] a) H. X. Dai, S. P. Yao, J. Wang, *Biotechnol. Lett.* **2006**, *28*, 1503–1507; b) B.-H. Xie, Z. Guan, Y.-H. He, *J. Chem. Technol. Biotechnol.* **2012**, *87*, 1709–1714.

[16] B. Liu, X. Qian, Q. Wu, X. Lin, *Enzyme Microb. Technol.* **2008**, *43*, 375–380.

[17] L.-H. Zhou, N. Wang, W. Zhang, Z.-B. Xie, X.-Q. Yu, *J. Mol. Catal. B* **2013**, *91*, 37–43.

[18] a) L. A. M. Rossato, M. Morsali, E. Ruffini, P. Bertuzzi, S. Serra, P. D'Arrigo, M. Sipponen, *ChemSusChem* **2024**, *17*, e2023008; b) M. Morsali, A. Moreno, A. Loukovitou, I. Pylypchuk, M. H. Sipponen, *Biomacromolecules* **2022**

[19] a) E. Tomaino, E. Capecchi, V. Ubertini, D. Piccinino, B. M. Bizzarri, R. Saladino, *J. Org. Chem.* **2024**, *89*(4), 2343–2350; b) D. Piccinino, V. Ubertini, E. Capecchi, E. Tomaino, V. Gigli, R. Saladino, *ChemCatChem* **2023**, *15*, e202300533; c) E. Capecchi, D. Piccinino, C. Nascimben, E. Tomaino, N. Ceccotti Vlas, S. Gabellone, R. Saladino, *Int. J. Mol. Sci.* **2023**, *24*, 9044; d) E. Tomaino, E. Capecchi, D. Piccinino, R. Saladino, *ChemCatChem* **2022**, e202200380; e) C. Tortolini, E. Capecchi, F. Tasca, R. Pofi, M. A. Venneri, R. Saladino, R. Antiochia, *Nanomaterials* **2021**, *11*, 718; f) E. Capecchi, D. Piccinino, B. M. Bizzarri, D. Avitabile, C. Pelosi, C. Colantonio, G. Calabrò, R. Saladino, *Biomacromolecules* **2019**, *20*, 1975–1988; g) D. Piccinino, E. Capecchi, L. Botta, P. Bollella, R. Antiochia, M. Crucianelli, R. Saladino, *Catal. Sci. Technol.* **2019**, *9*, 4125–4134; h) E. Capecchi, D. Piccinino, I. Delfino, P. Bollella, R. Antiochia, R. Saladino, *Nanomaterials* **2018**, *8*, 438.

[20] M. Sankar, E. Nowicka, E. Carter, D. M. Murphy, D. W. Knight, D. Bethell, G. J. Hutchings, *Nat. Commun.* **2014**, *5*, 3332.

[21] a) B. Maji, M. Baidya, J. Ammer, S. Kobayashi, P. Mayer, A. R. Ofial, H. Mayr, *Eur. J. Org. Chem.* **2013**, 3369–3377; b) M. S. Busch, E.-W. Knapp, *ChemPhysChem* **2004**, *5*, 1513–1522

[22] T. Wang, L. A. Liu, H. Wu, J. Zhang, Z. Feng, X. Yan, X. Wang, G. Han, X. Feng, L. Ren, X. Guo, *Dalton Trans.* **2024**, *53*, 5212–5221.

[23] a) J. Hermoso, D. Pignol, B. Kerfelec, I. Crenon, C. Chapus, J. C. Fontecilla-Camps, *J. Biol. Chem.* **1996**, *271*, 18007–18016; b) K. Laurvick, J. Srinivasan, *"Lipase From Mucor Javanicus" 89th JECFA - Chemical and Technical Assessment (CTA)*, **2020**.

[24] J. F. González, J. C. Menéndez, *Molecules* **2014**, *19*, 7317–7326.

[25] S. H. Son, Y. Y. Cho, H.-S. Yoo, S. J. Lee, Y. M. Kim, H. J. Jang, D. H. Kim, J.-W. Shinb, N.-J. Kim, *RSC Adv.* **2021**, *11*, 14000–14006.

[26] D. Kumar, G. Patel, A. K. Kumar, R. J. Roy, *Heterocycl. Chem.* **2009**, *46*, 791–795.

[27] a) T. Janeczko, M. Dymarska, M. Siepka, R. Gniłka, A. Lesniak, J. Popłonski, E. Kostrzewa-Susłow, *J. Mol. Catal. B Enzyme* **2014**, *109*, 47–52; b) T. Izumi, T. Hino, A. Kasahara, *J. Chem. Soc.-Perkin Trans.* **1992**, *1*, 1265–1267.

[28] J. Yang, J. Lai, W. Kong, S. Li, *J. Agric. Food Chem.* **2022**, *70*, 3409–3419.

[29] S. Ramadas, G. L. D. Krupadanam, *Tetrahedron: Asymmetry* **2004**, *15*, 3381–3391.

[30] H.-F. Wang, H. Xiao, X.-W. Wang, G. Zhao, *Tetrahedron* **2011**, *67*, 5389–5394.

[31] a) H. Zhang, R. Zhu, Y. Shi, X. Yu, L. Zhang, Y. Li, G. Shi, *Ind. Crops Prod.* **2023**, *193*, 116241; b) M. Stanisz, K. Bachosz, K. Siwi'nska-Ciesielczyk, Ł. Klapiszewski, J. Zdarta, T. Jesionowski, *Catalysts* **2022**, *12*, 1031.

[32] a) E. Capecchi, D. Piccinino, E. Tomaino, B. M. Bizzarri, F. Polli, R. Antiochia, F. Mazzei, R. Saladino, *RSC Adv.* **2020**, *10*, 29031–29042; b) E. Capecchi, D. Piccinino, B. M. Bizzarri, L. Botta, M. Crucianelli, R. Saladino, *Catalysts* **2020**, *10*, 313; c) Y. Zhang, Y. Yong, J. Ge, Z. Liu, *ACS Catal.* **2016**, *6*, 3789–3795; d) Y. Yong, R. Su, X. Liu, W. Xu, Y. Zhang, R. Wang, P. Ouyang, J. Wu, J. Ge, Z. Liu, *Biochem. Eng. J.* **2018**, *129*, 26–32; e) G. van Schaick, S. Pot, O. Schouten, J. Den Hartog, M. Akeroyd, R. van der Hoeven, W. Bijleveld, N. Abello, M. Wuhrer, M. Olsthoorn, E. Dominguez-Vega, *Food Chem.* **2023**, *421*, 136147; f) J. Fu, Y. R. Yang, A. Johnson-Buck, M. Liu, Y. Liu, N. G. Walter, N. W. Woodbury, H. Yan, *Nat. Nanotechnol.* **2014**, *9*, 531–536.

[33] X. Meng, C. Crestini, H. Ben, N. Hao, Y. Pu, A. J. Ragauskas, D. S. Argyropoulos, *Nat. Protoc.* **2019**, *14*, 2627–2647.

[34] a) S. K. Verma, K. K. Ghosh, R. Verma, S. Verma, *Int. J. Chem. Kinet.* **2021**, *53*, 308–316; b) D. M. Scheibel, I. Gitsov, *Biomacromolecules* **2019**, *20*, 927–936.

[35] J. Fu, Y. R. Yang, A. Johnson-Buck, M. Liu, Y. Liu, N. G. Walter, N. W. Woodbury, H. Yan, *Nat. Nanotechnol.* **2014**, *9*, 531–536.

[36] R. Kumar, *J. Cell. Biochem.* **2023**, *124*, 877–888.

[37] B. Webb, A. Sali, *Curr. Protoc. Bioinforma.* **2016**, *54*, 5.6.1–5.6.37.

[38] a) J. Jumper, R. Evans, A. Pritzel, T. Green, M. Figurnov, O. Ronneberger, K. Tunyasuvunakool, R. Bates, A. Žídek, A. Potapenko, A. Bridgland, C. Meyer, S. A. A. Kohl, A. J. Ballard, A. Cowie, B. Romera-Paredes, S. Nikolov, R. Jain, J. Adler, T. Back, S. Petersen, D. Reiman, E. Clancy, M. Zielinski, M. Steinegger, M. Pacholska, T. Berghammer, S. Bodenstein, D. Silver, O. Vinyals, A. W. Senior, K. Kavukcuoglu, P. Kohli, D. Hassabis, *Nature* **2021**, *596*, 583–589; b) M. Mirdita, K. Schütze, Y. Moriwaki, L. Heo, S. Ovchinnikov, M. Steinegger, *Nat. Methods.* **2022**, *6*, 679–682.

[39] a) M. Baek, F. DiMaio, I. Anishchenko, J. Dauparas, S. Ovchinnikov, G. R. Lee, J. Wang, Q. Cong, L. N. Kinch, R. D. Schaeffer, C. Millán, H. Park, C. Adams, C. R. Glassman, A. DeGiovanni, J. H. Pereira, A. V. Rodrigues, A. A. van Dijk, A. C. Ebrecht, D. J. Opperman, T. Sagmeister, C. Buhlheller, T. Pavkov-Keller, M. K. Rathinaswamy, U. Dalwadi, C. K. Yip, J. E. Burke, K. C. Garcia, N. V. Grishin, P. D. Adams, R. J. Read, D. Baker, *Science* **2021**, *373*, 871–876; b) I. R. Humphreys, J. Pei, M. Baek, A. Krishnakumar, I. Anishchenko, S. Ovchinnikov, J. Zhang, T. J. Ness, S. Banjade, S. R. Bagde, V. G. Stancheva, X.-H. Li, K. Liu, Z. Zheng, D. J. Barrero, U. Roy, J. Kuper, I. S. Fernández, B. Szakal, D. Branzei, J. Rizo, C. Kisker, E. C. Greene, S. Biggins, S. Keeney, E. A. Miller, J. C. Fromme, T. L. Hendrickson, Q. Cong, D. Baker, *Science* **2021**.

[40] X. Zhou, W. Zheng, Y. Li, R. Pearce, C. Zhang, E. W. Bell, G. Zhang, Y. Zhang, *Nat. Protoc.* **2022**, *17*, 2326–2353.

[41] R. A. Laskowski, M. W. MacArthur, D. S. Moss, J. M. Thornton, *J. Appl. Crystallogr.* **1993**, *26*, 283–291.

[42] C. Colovos, T. O. Yeates, *Protein Sci.* **1993**, *9*, 1511–1519.

[43] a) J. U. Bowie, R. Lüthy, D. Eisenberg, *Science* **1991**, *253*, 164–70; b) R. Lüthy, J. U. Bowie, D. Eisenberg, *Nature* **1992**, *356*, 83–85.

[44] a) M. Wiederstein, M. J. Sippl, *Nucleic Acids Res.* **2007**, *35*, 407–410; b) M. J. Sippl, *Proteins* **1993**, *17*, 355–62.

[45] G. Studer, M. Biasini, T. Schwede, *Bioinformatics* **2014**, *30*, 505–511.

[46] S. Pronk, S. Páll, R. Schulz, P. Larsson, P. Bjelkmar, R. Apostolov, M. R. Shirts, J. C. Smith, P. M. Kasson, D. van der Spoel, B. Hess, E. Lindahl, *Bioinformatics* **2013**, *29*, 845–854.

[47] W. Tian, C. Chen, X. Lei, J. Zhao, J. Liang, *Nucleic Acids Res.* **2018**, *46*, 363–367.
[48] a) J. Eberhardt, D. Santos-Martins, A. F. Tillack, S. Forli, *J. Chem. Inf. Model.* **2021**, *61*, 3891–3898; b) O. Trott, A. J. Olson, *J. Comput. Chem.* **2010**, *31*, 455–461.
[49] S. Salentin, S. Schreiber, V. J. Haupt, M. F. Adasme, M. Schroeder, *Nucleic Acids Res.* **2015**, *43*, 443–447.
[50] S. T. Ngo, *Methods Mol. Biol.* **2022**, *2385*, 313–323.
[51] E. Chovancova, A. Pavelka, P. Benes, O. Strnad, J. Brezovsky, B. Kozlikova, A. Gora, V. Sustr, M. Klvana, P. Medek, L. Biedermannova, J. Sochor, J. Damborsky, *PLoS Comput. Biol.* **2012**, *8*, e1002708.
[52] R. K. Singh, M. K. Tiwari, R. Singh, J.-K. Lee, *Int. J. Mol. Sci.* **2013**, *14*, 1232–1277.
[53] J. M. Palomo, R. L. Segura, C. Mateo, M. Terreni, J. M. Guisana, R. Fernàndez-Lafuentea, *Tetrahedron: Asymmetry* **2005**, *16*, 869–874.
[54] G. Fernàndez-Lorente, J. M. Palomo, C. Mateo, R. Munilla, C. Ortiz, Z. Cabrera, J. M. Guisàn, R. Fernàndez-Lafuente, *Biomacromolecules* **2006**, *7*, 2610–2615.
[55] D. Batovska, S. Parushev, A. Slavova, V. Bankova, I. Tsvetkova, M. Ninova, H. Najdenski, *Eur. J. Med. Chem.* **2007**, *42*, 87–92.
[56] J. Huang, *J. Comput. Chem.* **2013**, *34*, 2135–2145.
[57] a) S. Jo, T. Kim, V. G. Iyer, W. Im, *J. Comput. Chem.* **2008**, *29*, 1859–1865; b) S. Kim, J. Lee, S. Jo, C. L. Brooks III, H. S. Lee, W. Im, *J. Comput. Chem.* **2017**, *38*, 1879–1886.
[58] P. Mark, N. Lennart, *J. Phys. Chem.* **2001**, *105*, 9954–9960.
[59] a) T. Castrignanò, S. Gioiosa, T. Flati, M. Cestari, E. Picardi, M. Chiara, M. Fratelli, S. Amente, M. Cirilli, M. A. Tangaro, G. Chillemi, G. Pesole, F. Zambelli, *BMC Bioinf.* **2020**, *21*, 352; b) J. Di Martino, M. Arcieri, F. Madeddu, M. Pieroni, G. Carotenuto, P. Bottoni, L. Botta, T. Castrignanò, S. Gabellone, R. Saladino, *Int. J. Mol. Sci.* **2024**, *25*, 234; c) F. Madeddu, J. Di Martino, M. Pieroni, D. Del Buono, P. Bottoni, L. Botta, T. Castrignanò, R. Saladino, *Int. J. Mol. Sci.* **2022**, *23*, 14652.
[60] M. Pieroni, F. Madeddu, J. Di Martino, M. Arcieri, V. Parisi, P. Bottoni, T. Castrignanò, *Int. J. Mol. Sci.* **2023**, *24*, 11671.
[61] N. Mameda, S. Peraka, S. Kodumuri, D. Chevella, R. Banothu, V. Amruthamb, N. Nama, *RSC Adv.* **2016**, *6*, 58137–58141.
[62] I. Kostopoulou, A. Tzani, N.-I. Polyzos, M.-A. Karadendrou, E. Kritsi, E. Pontiki, T. Liargkova, D. Hadjipavlou-Litina, P. Zoumpoulakis, A. Detsi, *Molecules* **2021**, *26*, 2777.
[63] C. A. Slabber, C. D. Grimmer, O. Q. Munro, R. S. Robinson, *J. Chem. Crystallogr.* **2018**, *48*, 213–219.
[64] V. A. Adole, P. B. Koli, R. A. Shinde, R. S. Shinde, *Mat. Sci. Res. India* **2020**, *17*, 41–53.
[65] D. Zhao, B. Beiring, F. Glorius, *Angew. Chem. Int. Ed.* **2013**, *52*, 8454–8458.
[66] A. Lobley, M. I. Sadowski, D. T. Jones, *Bioinformatics* **2009**, *25*, 1761–1767.
[67] D. E. Kim, D. Chivian, D. Baker, *Nucleic Acids Res.* **2004**, *32*, 526–531.

Manuscript received: June 7, 2024
Revised manuscript received: July 19, 2024
Accepted manuscript online: August 20, 2024
Version of record online: October 16, 2024